

TN 1288

# NATIONAL ADVISORY COMMITTEE FOR AERONAUTICS

TECHNICAL NOTE

No. 1288



FLIGHT TESTS OF AN AIRPLANE MODEL WITH A  $62^{\circ}$  SWEEPED-BACK  
WING IN THE LANGLEY FREE-FLIGHT TUNNEL

By Bernard Maggin and Charles V. Bennett

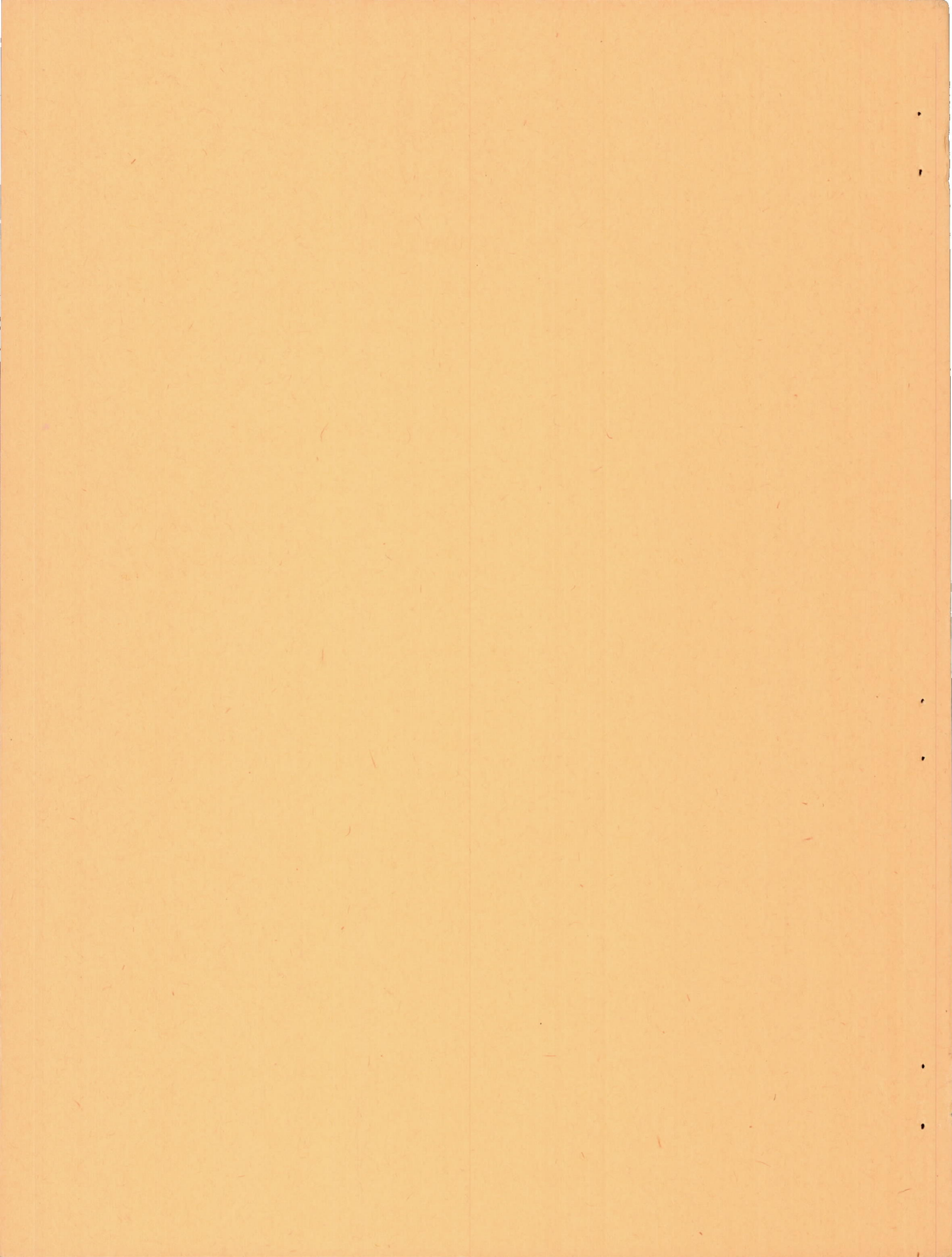
Langley Memorial Aeronautical Laboratory  
Langley Field, Va.

TECHNICAL LIBRARY  
AIRESEARCH MANUFACTURING CO.  
9651-9951 SEPULVEDA BLVD.  
INGLEWOOD,  
CALIFORNIA



Washington

May 1947



NATIONAL ADVISORY COMMITTEE FOR AERONAUTICS

TECHNICAL NOTE NO. 1288

FLIGHT TESTS OF AN AIRPLANE MODEL WITH A  $62^\circ$  SWEEP-BACK

WING IN THE LANGLEY FREE-FLIGHT TUNNEL

By Bernard Maggin and Charles V. Bennett

SUMMARY

A flight investigation has been made in the Langley free-flight tunnel to determine the severity of the dynamic stability and control problems associated with  $62^\circ$  sweepback. In the investigation a simplified model having a  $62^\circ$  swept-back wing of aspect ratio 2.5 and taper ratio 0.5 was used. In addition to the flight tests, force tests and tuft tests were made to determine the static-stability and wing-stall characteristics, and calculations were made to determine the boundary of zero damping of the lateral oscillation.

The model was successfully flown over a limited range of lift coefficients and, in general, the results indicated that the problems associated with  $62^\circ$  sweepback were similar to those previously found to be associated with  $42^\circ$  sweepback. The particular model wing used was found to be statically unstable longitudinally at high lift coefficients when tested alone, but the addition of a horizontal tail resulted in satisfactory longitudinal stability except between lift coefficients of 0.65 and 0.70 at which difficulty was encountered in flight in establishing the correct tunnel airspeed and glide angle.

The lateral oscillations of the model appeared to be well damped even for conditions which calculations indicated were unstable. The large value of rolling moment due to sideslip affected the controllability adversely, particularly when the directional stability was low. These results indicated that, at least for airplanes of low relative density, the dihedral and vertical-tail design will be determined more from considerations of controllability than of dynamic lateral stability. The lateral control became weaker with increasing angle of attack, and flights could not be made at lift coefficients greater than 0.88 because of insufficient lateral control.

## INTRODUCTION

Some of the stability and control problems associated with swept-back wings on aircraft are discussed in reference 1. In order to determine the significance and solution of some of these problems in terms of actual flight behavior, a program of research has been undertaken in the Langley free-flight tunnel with a series of swept-wing models. Damping-in-roll measurements for wings having  $2^\circ$ ,  $42^\circ$ , and  $62^\circ$  sweepback are given in reference 2, and the low-speed stability and damping in roll for a series of wings of different aspect ratio for  $42^\circ$  sweepback and  $38^\circ$  sweepforward are given in reference 3. The effect of aspect ratio on longitudinal stability at the stall has been analyzed and is discussed in reference 4. The flight behavior of a complete model having the  $42^\circ$  swept-back wing of reference 1 was determined in the Langley free-flight tunnel and is discussed in reference 5. In the tests of reference 5 it was found that, in general, the problems indicated in reference 1 existed, although the problem of obtaining stable lateral oscillations was not so difficult as was indicated. In addition, however, at a lift coefficient of approximately 0.7 the dynamic longitudinal behavior was found to be unsatisfactory and appeared to be associated with flow changes over the high-aspect-ratio wing used. In order to extend this work to higher sweep angles, an investigation was undertaken in the Langley free-flight tunnel with a model having the  $62^\circ$  swept-back wing of reference 2. The wing aspect ratio was 2.5, the taper ratio was 0.50, and the relative density of the complete model was 9.69. Force tests, flight tests, and tuft tests were made, and the results are given herein.

The flight tests were made at lift coefficients from 0.34 to 0.88 with various amounts of directional stability. Force tests were made to determine the static stability characteristics of the wing alone and of the complete model with various sizes and locations of the vertical tail. In addition, calculations were made to determine the boundary of zero damping of the lateral oscillations of the model to obtain a correlation with the flight-test results.

## SYMBOLS

The forces and coefficients were measured about the stability axes. A diagram of these axes showing positive direction of the forces and moments is given as figure 1.

S wing area, square feet

- W weight of model, pounds
- V airspeed, feet per second
- l tail length, feet
- b wing span, feet
- c wing chord unless otherwise noted, feet; measured in plane parallel to plane of symmetry
- $\bar{c}$  mean aerodynamic chord, feet; measured in plane parallel to plane of symmetry  $\left( \frac{2}{S} \int_0^{b/2} c^2 db \right)$
- $\Lambda$  angle of sweepback of quarter-chord line of wing, degrees
- i incidence, degrees
- $\alpha$  angle of attack, degrees
- $\lambda$  taper ratio  $\left( \frac{c_T}{c_r} \right)$
- $\delta_r$  rudder deflection, degrees
- $\delta_e$  elevator deflection, degrees
- M pitching moment, foot-pounds
- L rolling moment, foot-pounds
- N yawing moment, foot-pounds
- $C_L$  lift coefficient  $\left( \frac{\text{Lift}}{qS} \right)$
- $C_D$  drag coefficient  $\left( \frac{\text{Drag}}{qS} \right)$
- $C_m$  pitching moment coefficient  $\left( \frac{M}{qS\bar{c}} \right)$

- $C_l$  rolling-moment coefficient  $\left(\frac{L}{qSb}\right)$
- $C_n$  yawing-moment coefficient  $\left(\frac{N}{qSb}\right)$
- $C_Y$  lateral-force coefficient  $\left(\frac{\text{Lateral force}}{qS}\right)$
- $\rho$  mass density of air at standard conditions, slugs per cubic foot
- $q$  dynamic pressure, pounds per square foot
- $\beta$  angle of sideslip, degrees
- $\gamma$  flight-path angle, degrees
- $\psi$  angle of yaw, degrees (for force-test data,  $\psi = -\beta$ )
- $\phi$  angle of roll, degrees
- $\Delta\delta_a \left(\frac{pb}{2V} = .05\right)$  total aileron deflection (sum of deflections of right and left ailerons equal up and down) required to produce a value of  $\frac{pb}{2V}$  of 0.05, degrees
- $\frac{rb}{2V}$  yawing angular velocity
- $\frac{pb}{2V}$  helix angle generated by wing tip (rolling-velocity factor)
- $C_{l\delta_a}$  rolling-moment coefficient per degree deflection of one aileron  $\left(\frac{\partial C_l}{\partial \delta_a}\right)$
- $\mu$  relative-density factor  $\left(\frac{m}{\rho S b}\right)$
- $m$  mass  $\left(\frac{W}{g}\right)$

- $g$  acceleration due to gravity (32.2 feet per second per second)
- $k_X$  radius of gyration about principal X-axis, feet
- $k_Z$  radius of gyration about principal Z-axis, feet
- $C_{l\beta}$  effective-dihedral parameter; rate of change of rolling-moment coefficient with angle of sideslip, per degree  

$$\left( \frac{\partial C_l}{\partial \beta} \right)$$
- $C_{n\beta}$  directional-stability parameter; rate of change of yawing-moment coefficient with angle of sideslip, per degree  

$$\left( \frac{\partial C_n}{\partial \beta} \right)$$
- $C_{np}$  rate of change of yawing-moment coefficient with rolling-angular-velocity factor  

$$\left( \frac{\partial C_n}{\partial \frac{pb}{2V}} \right)$$
- $C_{lp}$  rate of change of rolling-moment coefficient with rolling-angular-velocity factor  

$$\left( \frac{\partial C_l}{\partial \frac{pb}{2V}} \right)$$
- $C_{lr}$  rate of change of rolling-moment coefficient with yawing-angular-velocity factor  

$$\left( \frac{\partial C_l}{\partial \frac{rb}{2V}} \right)$$
- $C_{nr}$  rate of change of yawing-moment coefficient with yawing-angular-velocity factor  

$$\left( \frac{\partial C_n}{\partial \frac{rb}{2V}} \right)$$

$C_{Y\beta}$  effective side-area parameter, rate of change of lateral-force coefficient with angle of sideslip  $\left(\frac{\partial C_Y}{\partial \beta}\right)$

R Routh's discriminant

Subscripts:

T tip

r root

t horizontal tail

#### APPARATUS

The flight tests were made in the Langley free-flight tunnel, a description of which is given in reference 6. The force tests were made on the free-flight-tunnel six-component balance which rotates in yaw with the model so that all forces and moments are measured about the stability axes. (See fig. 1.) A description of this balance is given in reference 7. A photograph of the model flying in the test section of the tunnel is shown as figure 2. Tuft tests of the model wing were made in the Langley 15-foot free-spinning tunnel.

The model consisted of a wooden boom upon which were mounted the swept-back wing together with horizontal and vertical stabilizing surfaces. (See fig. 3.) The wing had  $62^\circ$  sweepback of the quarter-chord line and a taper ratio of 0.50. The airfoil section used was a Rhode St. Genese 33 section perpendicular to the 0.50-chord line. This section was used in accordance with Langley free-flight-tunnel practice of using airfoil sections that obtain maximum lift coefficients in the low-scale tests approximately equal to that of a full-scale wing having conventional airfoil sections. The stabilizing surfaces were straight-taper unswept horizontal and vertical tails having NACA 0009 airfoil sections. Two vertical tails were tested on the model, one 10.6 percent of the wing area and one 5.25 percent of the wing area. The model was so constructed that the directional stability could be changed by varying the vertical-tail length. The geometric characteristics of the vertical tails and the vertical-tail lengths tested are shown in figure 3.

## TESTS AND CALCULATIONS

Force tests were made to determine the lift, drag, and pitching-moment characteristics through the lift range for the model wing alone and for the complete model with  $-5^\circ$  incidence of the horizontal tail. In addition, force tests were made at  $\pm 5^\circ$  yaw over the lift range with  $-10^\circ$  incidence of the horizontal tail to determine the lateral stability characteristics of the model wing and for the complete model with vertical tail 2 mounted in position 1 and vertical tail 1 in positions 1, 2, and 4. (See fig. 3.) All the force tests were made at a dynamic pressure of 3.0 pounds per square foot, which corresponds to a test Reynolds number of 336,000 based on the mean aerodynamic chord of 1.05 feet.

Tuft tests were made to study the flow pattern over the wing alone throughout the lift range. These tests were made at a dynamic pressure of 2.8 pounds per square foot, which corresponds to a test Reynolds number of 326,000. Photographs were taken of the tufts on the upper surface of the wing at angles of attack from  $-8^\circ$  to  $28^\circ$ .

Flight tests of the model with the center of gravity at 0.45c and 0.30c and with the incidence of the horizontal tail at  $-5^\circ$  and  $-10^\circ$  were made for a lift-coefficient range from 0.34 to 0.88. For these tests vertical tail 2 was mounted in position 1. (See fig. 3.) Flight tests were also made at a lift coefficient of approximately 0.6 with vertical tail 1 mounted in positions 1, 2, 3, and 4. In all flights, abrupt deflections of approximately  $\pm 18^\circ$  (total  $36^\circ$ ) of the ailerons,  $5^\circ$  of the rudder, and  $5^\circ$  of the elevator were used for controlling the model. A complete description of the flight-testing technique used in the Langley free-flight tunnel is given in reference 6. The behavior of the model in flight under the various test conditions was noted by visual observations and supplemented by motion-picture records.

Calculations were made by the method of reference 8 to determine the boundary of zero damping ( $R = 0$ ) of the lateral oscillations for a lift coefficient of 0.6 to obtain a correlation with the flight results. In the calculations, the product-of-inertia terms were included in the equations as described in reference 9. The aerodynamic, geometric, and mass characteristics used in the calculations are presented in table I. The mass characteristics of the model were obtained by measurements. The flight-path angle, trim airspeed, and angle of attack for the lift coefficient of 0.6 were obtained from flight tests. The values of  $C_{Y\beta}$  and  $C_{n\beta}$  (tail off) were obtained from force tests, and the values of the

damping-in-roll parameter  $C_{l_p}$  were obtained from the experimental data of reference 2. The values of the other stability parameters were estimated from the data of reference 10 with some consideration being given to the effect of sweepback on these parameters.

## RESULTS AND DISCUSSION

### Force Tests

Longitudinal stability.- The results of the force tests to determine the lift, drag, and pitching-moment characteristics of the wing alone and of the complete model are shown in figure 4. The data presented show that the wing alone had unsatisfactory static longitudinal stability characteristics at moderate and high lift coefficients as evidenced by the changes in the slope of the pitching-moment curve and particularly by the increasing nosing-up moments at lift coefficients greater than 0.6. The data also show that the addition of a horizontal tail resulted in static longitudinal stability up to an angle of attack of  $24^\circ$  corresponding to a lift coefficient of 0.84. Reference 5 and unpublished wind-tunnel data indicate that the static longitudinal stability of swept-back-wing airplanes is critically dependent upon horizontal-tail position. All the tests on the model having a  $62^\circ$  swept-back wing, however, were made with the horizontal tail in the position shown in figure 3. This position gave static longitudinal stability.

Lateral stability.- The results of force tests made to determine the lateral stability characteristics of the model are presented in figure 5 in the form of plots of the lateral-force parameter  $C_{Y_\beta}$ , directional-stability parameter  $C_{n_\beta}$ , and the effective-dihedral parameter  $C_{l_\beta}$  against angle of attack and lift coefficient. The data show that the model wing had a variation of  $C_{l_\beta}$  with lift coefficient similar to that of the  $42^\circ$  swept-back wing of reference 5. As in the case of the  $42^\circ$  swept-back wing, the addition of the vertical tail to the  $62^\circ$  swept-back wing reduced the variation of  $C_{l_\beta}$  with lift coefficient because the vertical tail moves downward with increasing angle of attack. The data also show that with tail off the model had approximately zero directional stability  $C_{n_\beta}$  throughout

the lift range. An increase in vertical-tail area or tail length increased the directional stability, as would be expected.

### Flow Surveys

The results of the flow surveys of the wing are presented in figure 6. These data indicate that the general flow characteristics throughout the lift range are similar to those noted for the  $42^\circ$  swept-back wing (see reference 5) except that the progression of the outflow at the higher lifts is much more gradual with increasing angle of attack for the  $62^\circ$  swept-back wing. The more gradual outflow of the  $62^\circ$  swept-back wing resulted in a less abrupt stall as evidenced by the lift curve of the  $62^\circ$  swept-back wing compared with that of the  $42^\circ$  swept-back wing. (See fig. 4 and reference 5.)

### Flight Tests

Longitudinal stability. - The dynamic longitudinal stability characteristics of the model with the center of gravity at  $0.45\bar{c}$  was considered satisfactory between lift coefficients of 0.35 to 0.65. In this lift-coefficient range the model flew steadily and all pitching motions seemed to be heavily damped.

In flights made at lift coefficients between 0.65 and 0.70 some difficulty was encountered in establishing the correct trim airspeed and tunnel angle (which corresponds to the model flight-path angle). At times these settings appeared to be correct, but the model would tend to rise or fall in the tunnel suddenly and without any apparent reason and thus require large changes in tunnel angle and airspeed to maintain flight. Often the changes required would be so large that they could not be made quickly enough to prevent the model from crashing.

This erratic longitudinal behavior was very similar to that noted in flight tests of the model with the  $42^\circ$  swept-back wing between lift coefficients of 0.65 and 0.80 (reference 5). As in the case of the  $42^\circ$  swept-back wing, this longitudinal flight behavior is believed to be the result of the change in flow over the wing at moderate lift coefficients (as indicated by the wing-alone pitching-moment curve of fig. 4) combined with the variation of the flight-path angle with lift coefficient. (See fig. 7.) This erratic flight behavior of the model in the tunnel indicates that although static longitudinal stability is provided by a horizontal tail, airplanes with wings having abrupt changes in pitching-moment characteristics might have unsatisfactory dynamic longitudinal

stability characteristics. The unsatisfactory longitudinal stability noted in the model flights might be evidenced in full-scale flight by difficulty in maintaining steady flight, which would be particularly dangerous at high lift coefficients.

As in the case of the  $42^\circ$  swept-back wing, moving the center of gravity forward 0.15c to increase the static margin (see fig. 8) did not result in an improvement in the longitudinal-flight behavior between lift coefficients of 0.65 and 0.70.

In flights at lift coefficients between 0.70 and 0.88 the longitudinal stability was considered fairly satisfactory in that steady flights could be made and all pitching motions were well damped. Flights were not possible at lift coefficients above 0.88 because of the lack of lateral control at these lift coefficients.

Lateral stability. - In the flights made with vertical tails 1 or 2 in position 1, the lateral stability characteristics were satisfactory throughout the lift range investigated (0.34 to 0.88). The lateral motions, predominantly rolling accompanied by a small amount of yawing, were well damped. In fact, the damping appeared to be almost deadbeat. When the length of tail 1 was reduced (position 1 to 2) no appreciable change occurred in the lateral stability characteristics of the model. The lateral motions still appeared to be well damped and it was very difficult for the pilot to start a lateral oscillation even though the model was rolled violently by means of the ailerons. Although the damping of the lateral oscillation was not noticeably reduced, the model was harder to control laterally because greater angles of sideslip were attained inadvertently, which in turn produced large rolling moments that opposed and at times overpowered the aileron control.

With tail 1 mounted in positions 3 and 4 it was impossible to obtain flights of any duration and the pilot was unable to ascertain the lateral stability characteristics of the model in detail, although in none of the flights was there any discernible oscillatory motion. During take-off or in flight, if the model sideslipped large rolling moments were produced which the pilot could not overcome with the rudder and aileron controls and the model rolled off and crashed into the tunnel wall. The roll-off was attributed to the low directional stability with these tail configurations combined with large effective dihedral of the  $62^\circ$  swept-back wing at the lift coefficient of 0.60. The low directional stability permitted large angles of sideslip to be reached and the large effective dihedral resulted in a large adverse rolling moment which opposed the aileron rolling moments and weakened the lateral control.

The calculated boundary for zero damping of the lateral oscillation is presented and correlated with flight-test results in figure 9. The calculated data, which predict instability for tail 1 in positions 2, 3, and 4, disagree with the flight-test results, which indicated stability for tail 1 in position 2 and which showed no unstable oscillations with tail 1 at positions 3 and 4 even though long flights were impossible with these tail positions (positions 3 and 4) as has been noted. The disagreement between the flight tests and the calculated boundary is attributed in part to the lack of experimental data on some of the rotary derivatives used in the calculations. For example, some recent unpublished experimental data taken in the Langley stability tunnel on one  $60^\circ$  swept-back wing showed that the derivative  $C_{n_p}$  varied in an unconventional manner with angle

of attack and, for moderate and high angles of attack, was of opposite sign to that normally used. Calculations indicate that such a change in the value of  $C_{n_p}$  in the present case would

cause the oscillatory-stability boundary to shift downward into the range of negative values of  $C_{n_\beta}$ . This change would bring the

calculations into better agreement with the flight tests. These results emphasize the need for more experimental data on the rotary derivatives of highly swept wings.

Lateral control. - In the flights made over the lift range tested the aileron rolling effectiveness was seen to vary appreciably. At low lift coefficients (0.34 to 0.40) the aileron control was considered satisfactory when the directional stability was adequate. Between lift coefficients of 0.40 and 0.50 the aileron control became progressively less effective. At lift coefficients from 0.50 to approximately 0.80 the ailerons became slightly more effective although never so powerful as at the lower lift coefficients. From lift coefficients of 0.80 to 0.88 the lateral control again became weaker and at lift coefficient greater than 0.88, flights were impossible because of the complete lack of lateral control. At the trim lift coefficient of approximately 0.50 the aileron effectiveness appeared to vary during flight. Changes in air flow over the wing in this lift-coefficient range are believed to be a contributing factor. Data from reference 1, showing the variation in aileron rolling effectiveness with lift coefficient for the wing tested, are presented in figure 10. These data, which were obtained from static tests and damping-in-roll tests, show changes in aileron rolling effectiveness with lift coefficient similar to those noted in the flight tests.

## CONCLUDING REMARKS

The results of force and flight tests of an airplane model with a  $62^\circ$  swept-back wing in the Langley free-flight tunnel are summarized as follows:

1. In general, the problems of obtaining satisfactory stability and control with the  $62^\circ$  swept-back wing were similar to those for the  $42^\circ$  swept-back wing although loss of aileron control at high lift appeared to be more serious.
2. A horizontal tail was effective in making a longitudinally unstable wing stable although objectionable dynamic motions were encountered at lift coefficients of 0.65 to 0.70 which were believed to be associated with the change in flow over the wing.
3. The lateral oscillations of the model appeared to be well damped even for conditions which calculations indicated were unstable. This disagreement was attributed in part to the lack of experimental data on some of the rotary derivatives used in the calculations.
4. At low and moderate lift coefficients, the lateral control of the model was satisfactory when the directional stability was adequate but was unsatisfactory with low directional stability because, in these cases, inadvertent sideslipping introduced rolling moments which at times overpowered the aileron rolling moments. This effect was especially bad for the model tested because of the large value of rolling moment due to sideslip associated with the swept-back wing. These results indicated that, at least for airplanes of low relative density, the dihedral and vertical-tail design will be determined more from considerations of controllability than of dynamic lateral stability.
5. As the lift coefficient was increased the lateral control became weaker and flights could not be made at lift coefficients above 0.88 because of insufficient lateral control.

Langley Memorial Aeronautical Laboratory  
National Advisory Committee for Aeronautics  
Langley Field, Va., December 19, 1946

## REFERENCES

1. Soulé, Hartley A.: Influence of Large Amounts of Wing Sweep on Stability and Control Problems of Aircraft. NACA TN No. 1088, 1946.
2. Bennett, Charles V., and Johnson, Joseph L.: Experimental Determination of the Damping in Roll and Aileron Rolling Effectiveness of Three Wings Having  $2^\circ$ ,  $42^\circ$ , and  $62^\circ$  Sweepback. NACA TN No. 1273, 1947.
3. Maggin, Bernard, and Bennett, Charles V.: Low-Speed Stability and Damping-in-Roll Characteristics of Some Highly Swept Wings. NACA TN No. 1286, 1947.
4. Shortal, Joseph A., and Maggin, Bernard: Effect of Sweepback and Aspect Ratio on Longitudinal Stability Characteristics of Wings at Low Speeds. NACA TN No. 1093, 1946.
5. Maggin, Bernard, and Bennett, Charles V.: Flight Tests of an Airplane Model with a  $42^\circ$  Swept-Back Wing in the Langley Free-Flight Tunnel. NACA TN No. 1287, 1947.
6. Shortal, Joseph A., and Osterhout, Clayton J.: Preliminary Stability and Control Tests in the NACA Free-Flight Wind Tunnel and Correlation with Full-Scale Flight Tests. NACA TN No. 810, 1941.
7. Shortal, Joseph A., and Draper, John W.: Free-Flight-Tunnel Investigation of the Effect of the Fuselage Length and the Aspect Ratio and Size of the Vertical Tail on Lateral Stability and Control. NACA ARR No. 3D17, 1943.
8. Zimmerman, Charles H.: An Analysis of Lateral Stability in Power-Off Flight with Charts for Use in Design. NACA Rep. No. 589, 1937.
9. Sternfield, Leonard: Effect of Product of Inertia on Requirements for Lateral Stability. NACA TN No. 1193, 1947.
10. Pearson, Henry A., and Jones, Robert T.: Theoretical Stability and Control Characteristics of Wings with Various Amounts of Taper and Twist. NACA Rep. No. 635, 1938.

TABLE I

CHARACTERISTICS OF AIRPLANE MODEL WITH  $62^\circ$  SWEEPED-BACK WING

USED IN THE CALCULATIONS OF THE BOUNDARY OF ZERO

DAMPING OF THE LATERAL OSCILLATIONS ( $R = 0$ )

[The principal axes of inertia are assumed to correspond to the body axes of the model]

$C_L$ . . . . .	0.6
$\alpha$ , deg . . . . .	17
W/S, lb/sq ft . . . . .	1.85
b, ft . . . . .	2.5
$\rho$ , slugs/cu ft . . . . .	0.002378
V, ft/sec . . . . .	49.6
$\mu$ . . . . .	9.69
$k_X$ , ft . . . . .	0.41
$k_Z$ , ft . . . . .	1.18
$C_{l_r}$ . . . . .	$0.156 - 0.383C_{n_{\beta_{tail}}}$
$C_{n_p}$ . . . . .	$-0.0445 - 0.383C_{n_{\beta_{tail}}}$
$C_{l_p}$ . . . . .	-0.15
$C_{n_r}$ . . . . .	$-0.0096 - 2\frac{l}{b}C_{n_{\beta_{tail}}}$
$C_{y_{\beta}}$ . . . . .	$-0.0015 - 0.95C_{n_{\beta_{tail}}}$
$C_{n_{\beta}}$ (wing and fuselage) . . . . .	0
$\gamma$ , deg . . . . .	-18

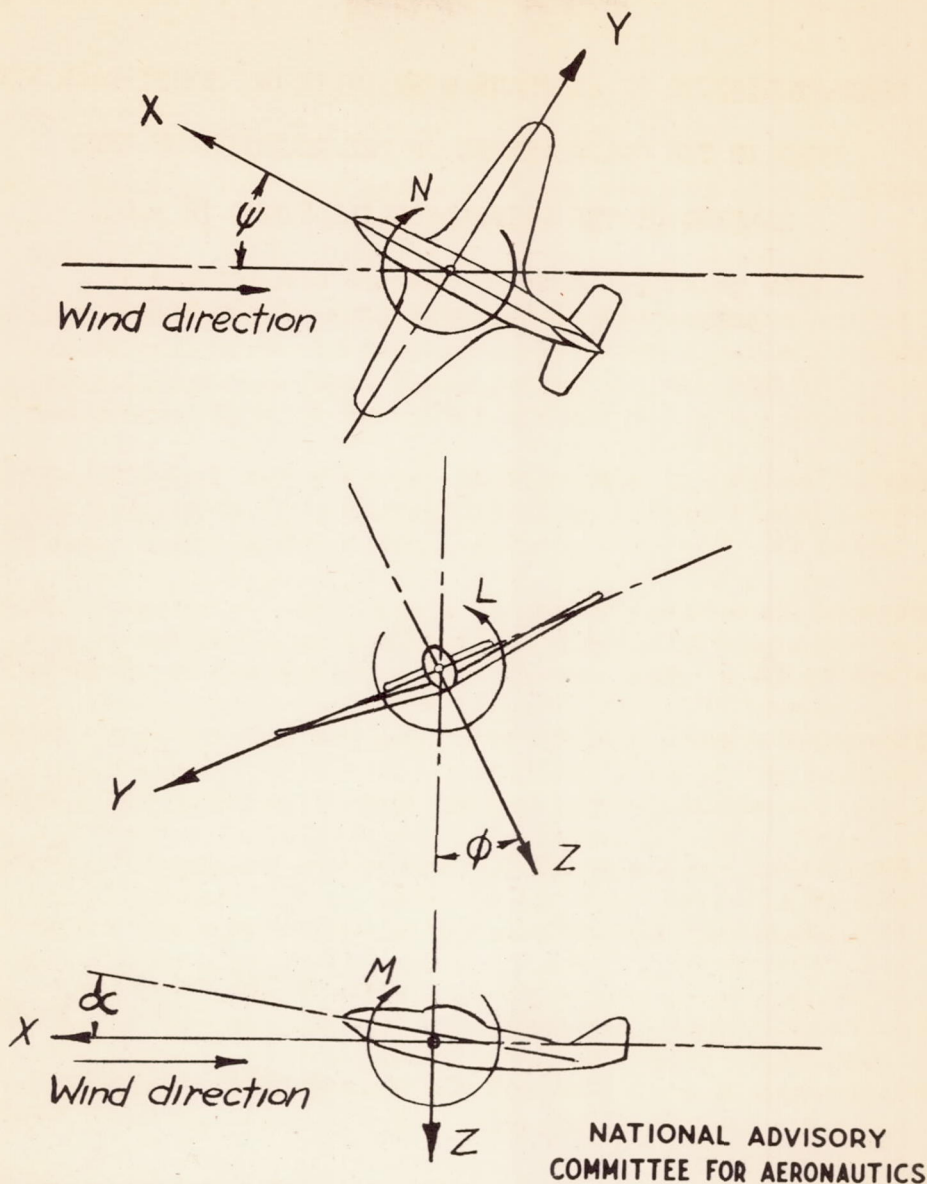
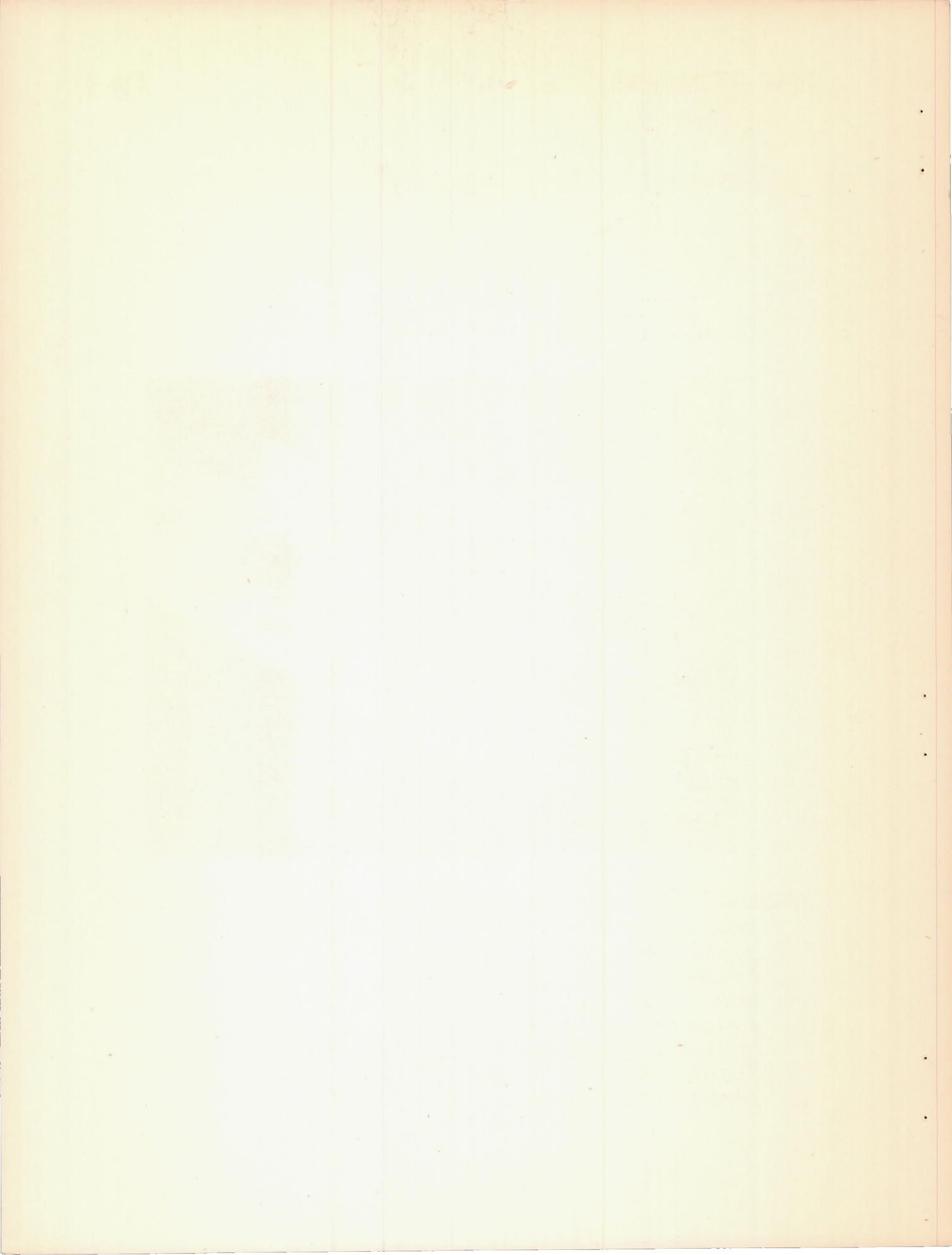


Figure 1.- The stability system of axes. Arrows indicate positive directions of moments and forces. This system of axes is defined as an orthogonal system having its origin at the center of gravity and in which the Z-axis is in the plane of symmetry and perpendicular to the relative wind, the X-axis is in the plane of symmetry and perpendicular to the Z-axis, and the Y-axis is perpendicular to the plane of symmetry.



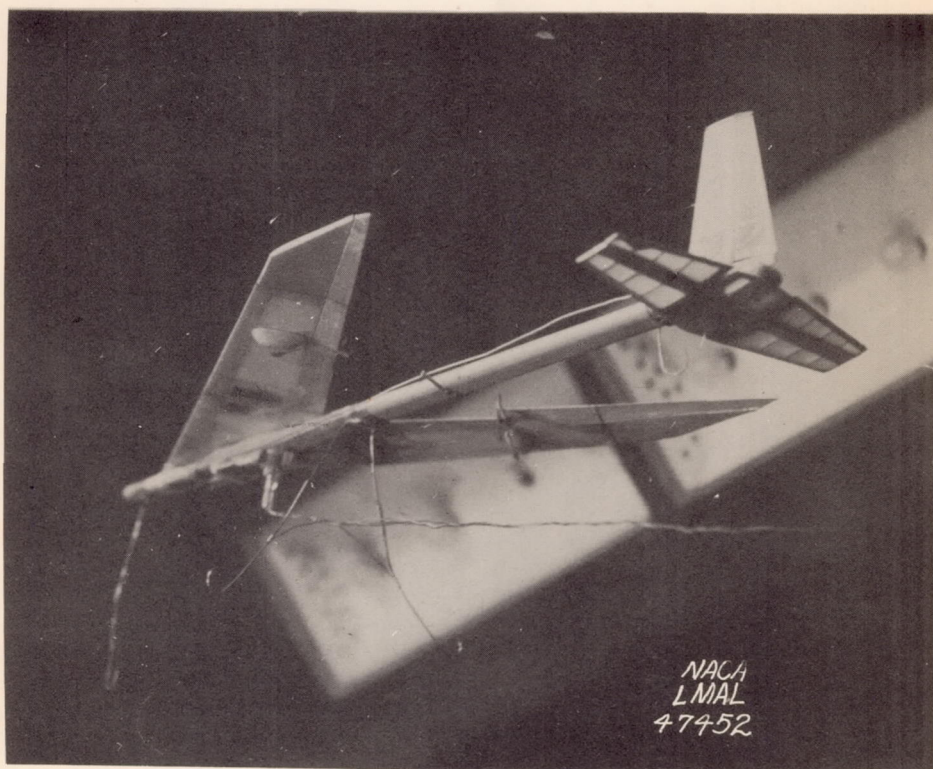


Figure 2.- Airplane model with  $62^{\circ}$  swept-back wing in flight in the Langley free-flight tunnel.



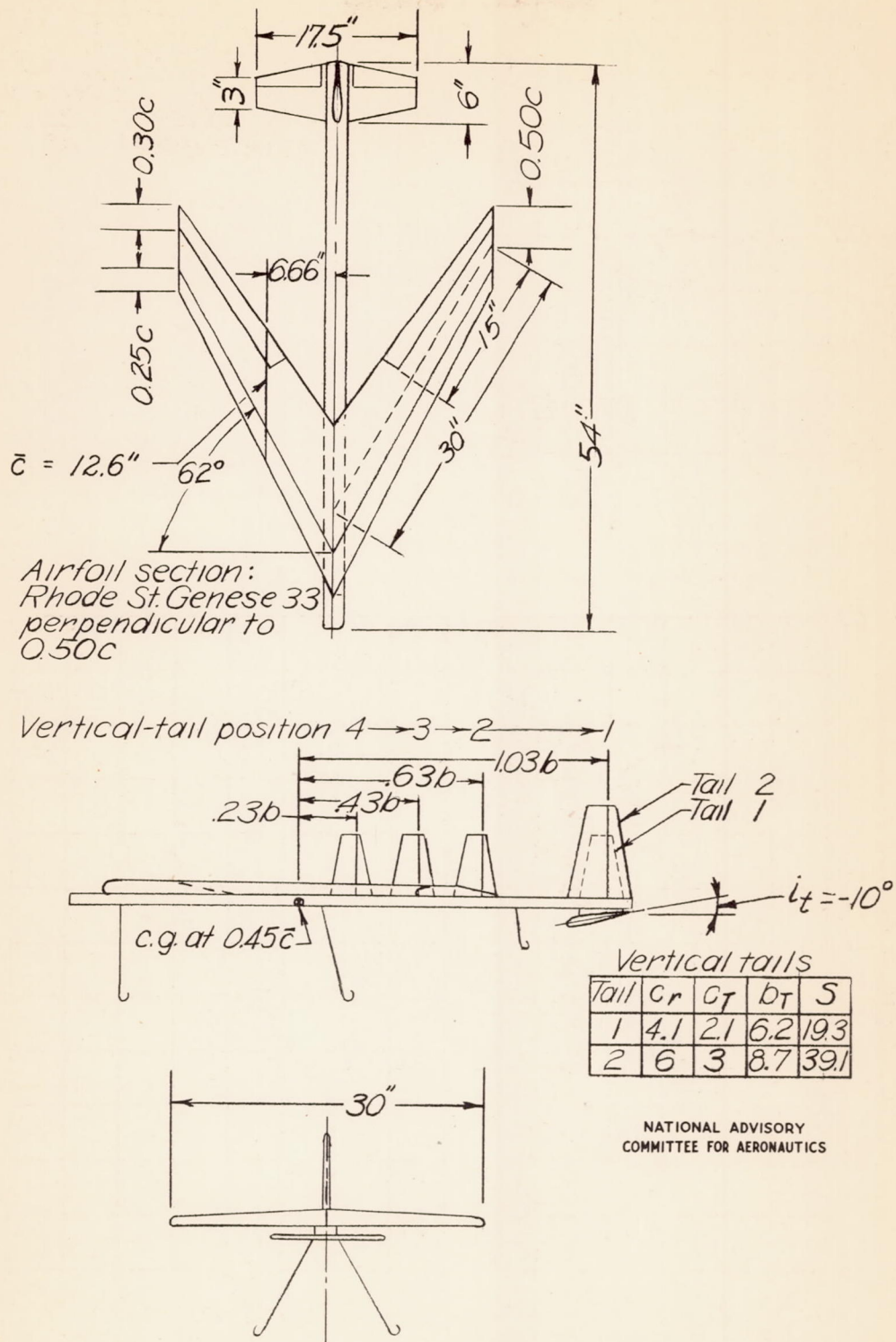


Figure 3.- Airplane model with 62° swept-back wing tested in Langley free-flight tunnel.  $C_r = 16.22$  inches;  $c_T = 8.11$  inches.

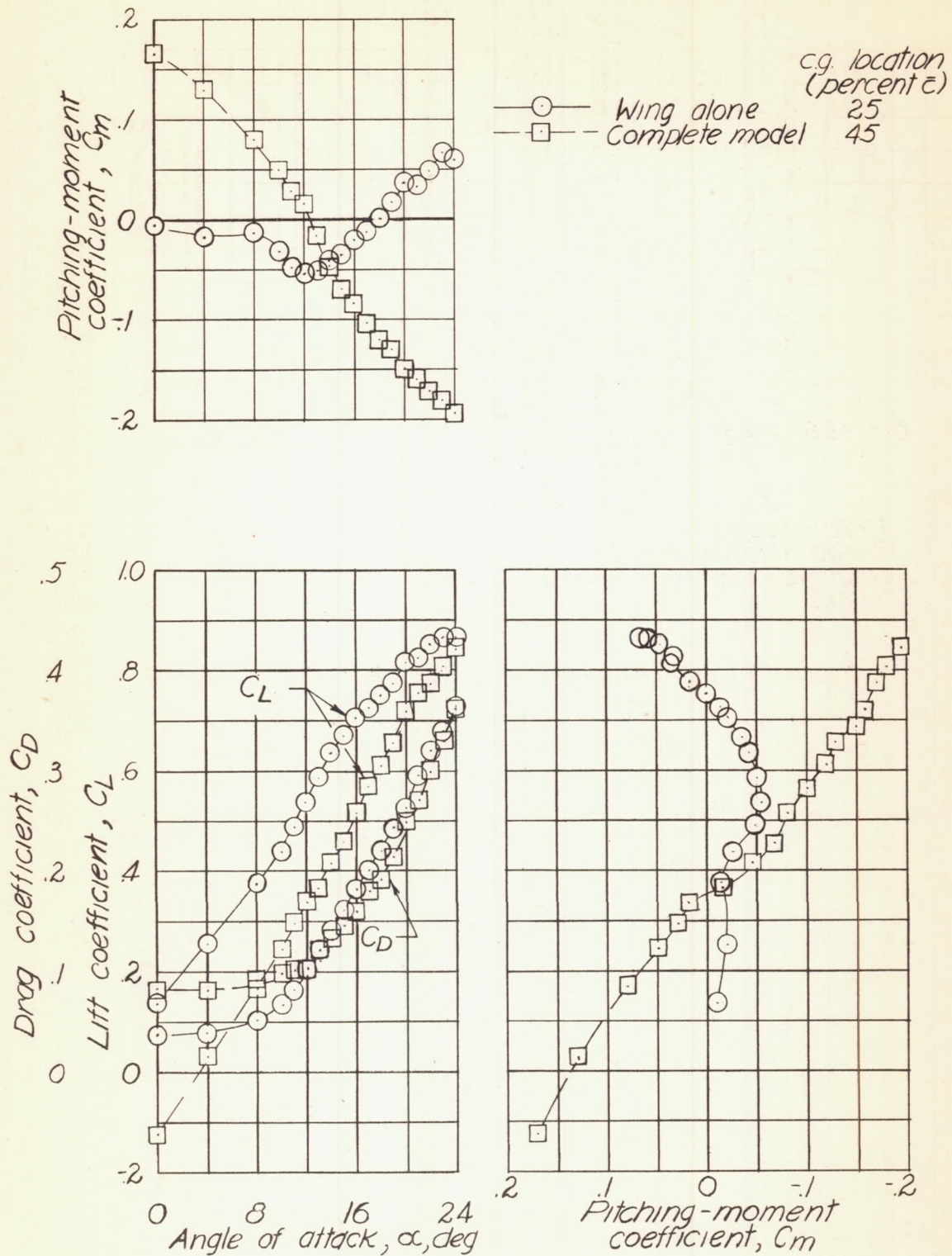


Figure 4.- The lift, drag, and pitching-moment characteristics of the 62° swept-back-wing airplane model and wing alone.  $q=3.0$ .

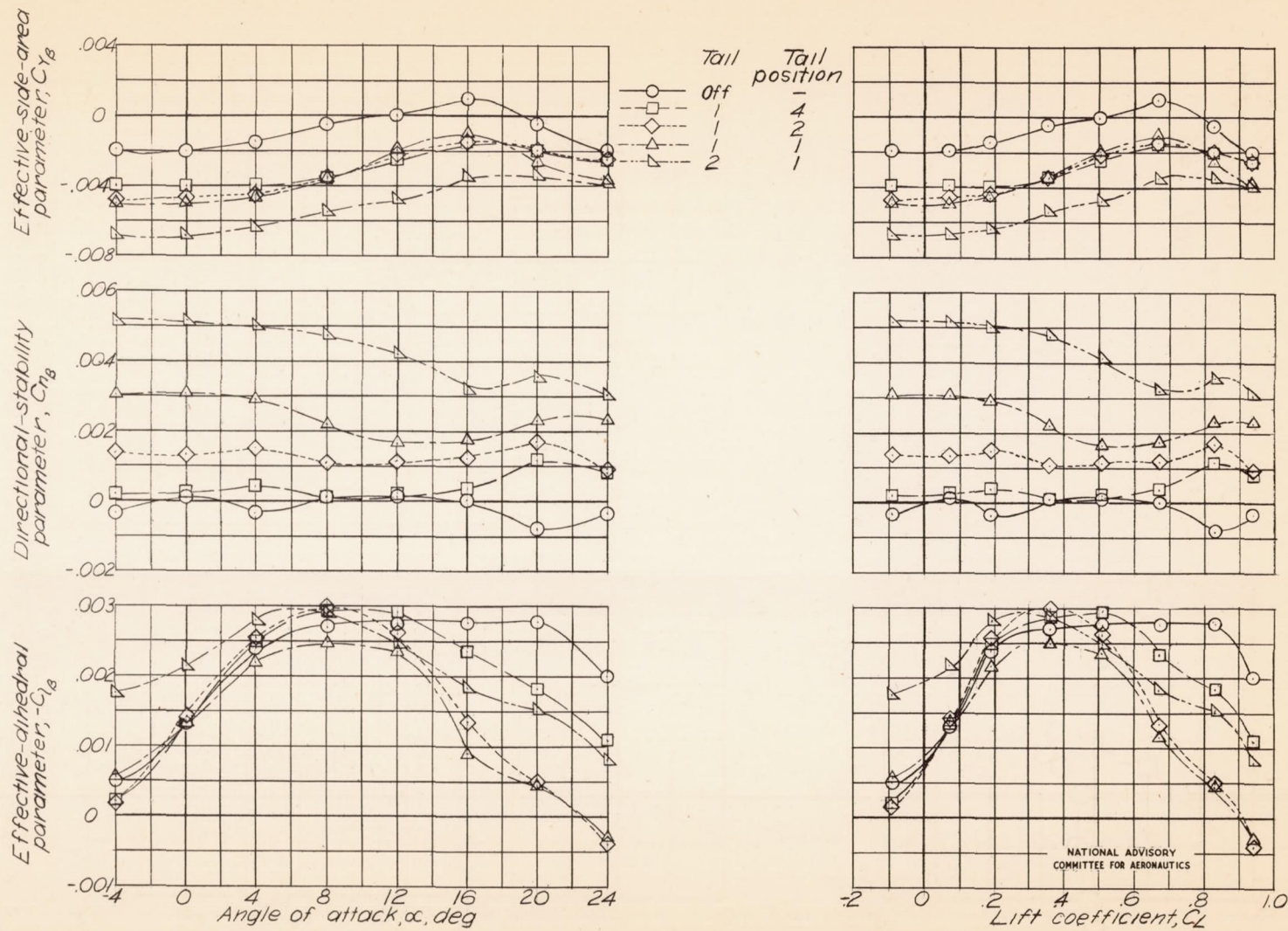


Figure 5—The lateral stability characteristics of the test model with various vertical-tail arrangements.



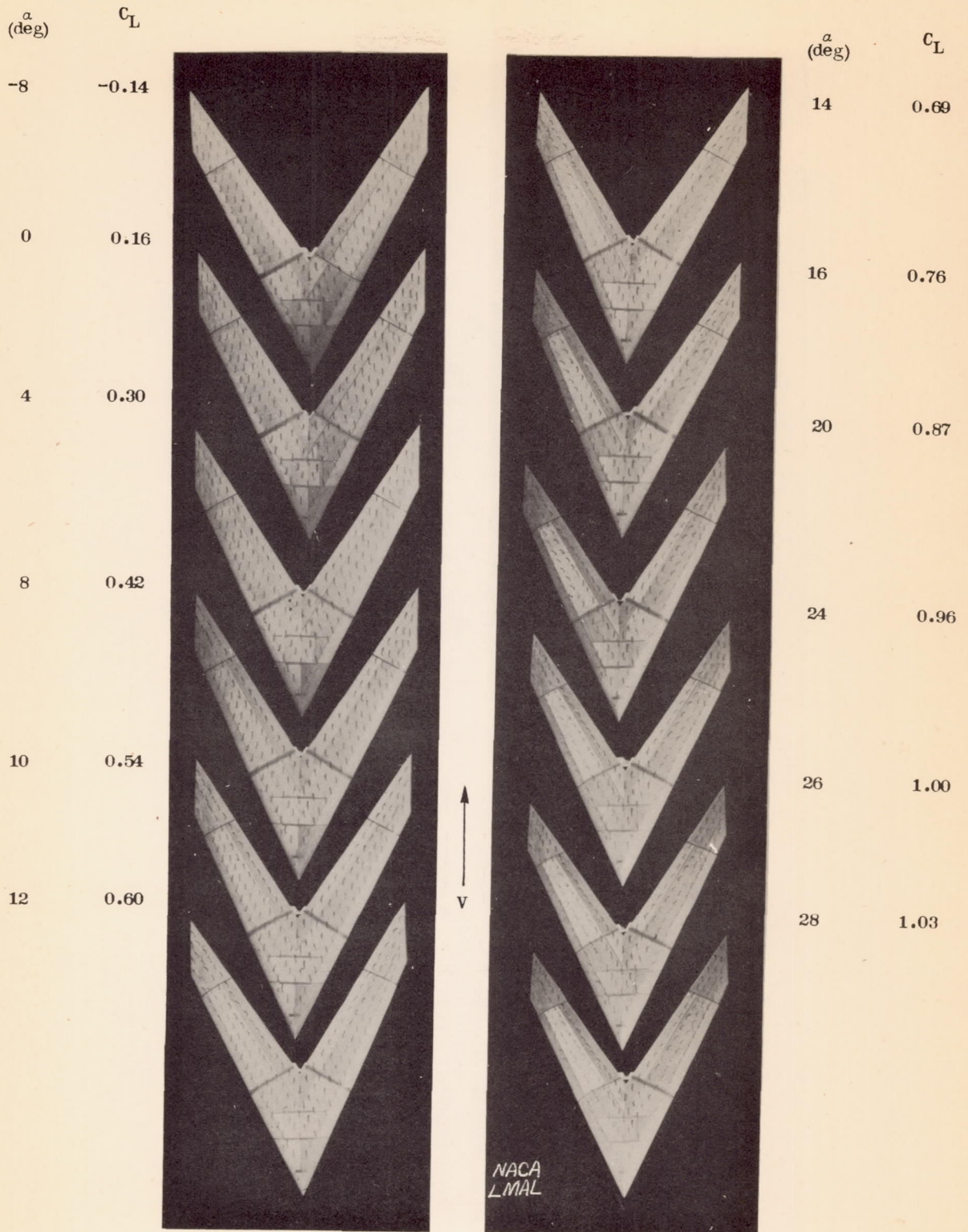


Figure 6.- Tuft studies of 62° swept-back wing.



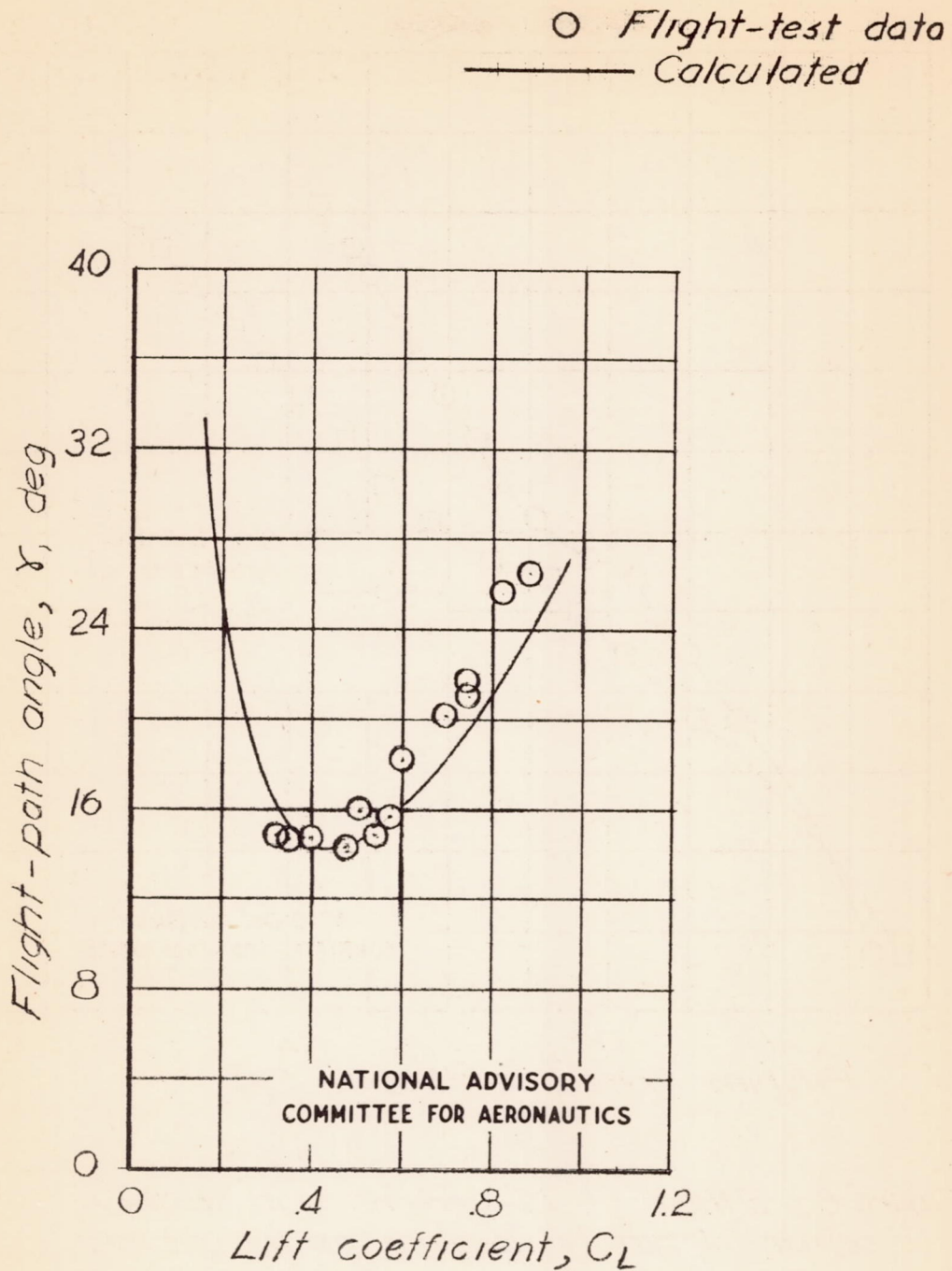


Figure 7.- Variation of the flight-path angle with lift coefficient obtained from flight tests and as calculated from force-test data.

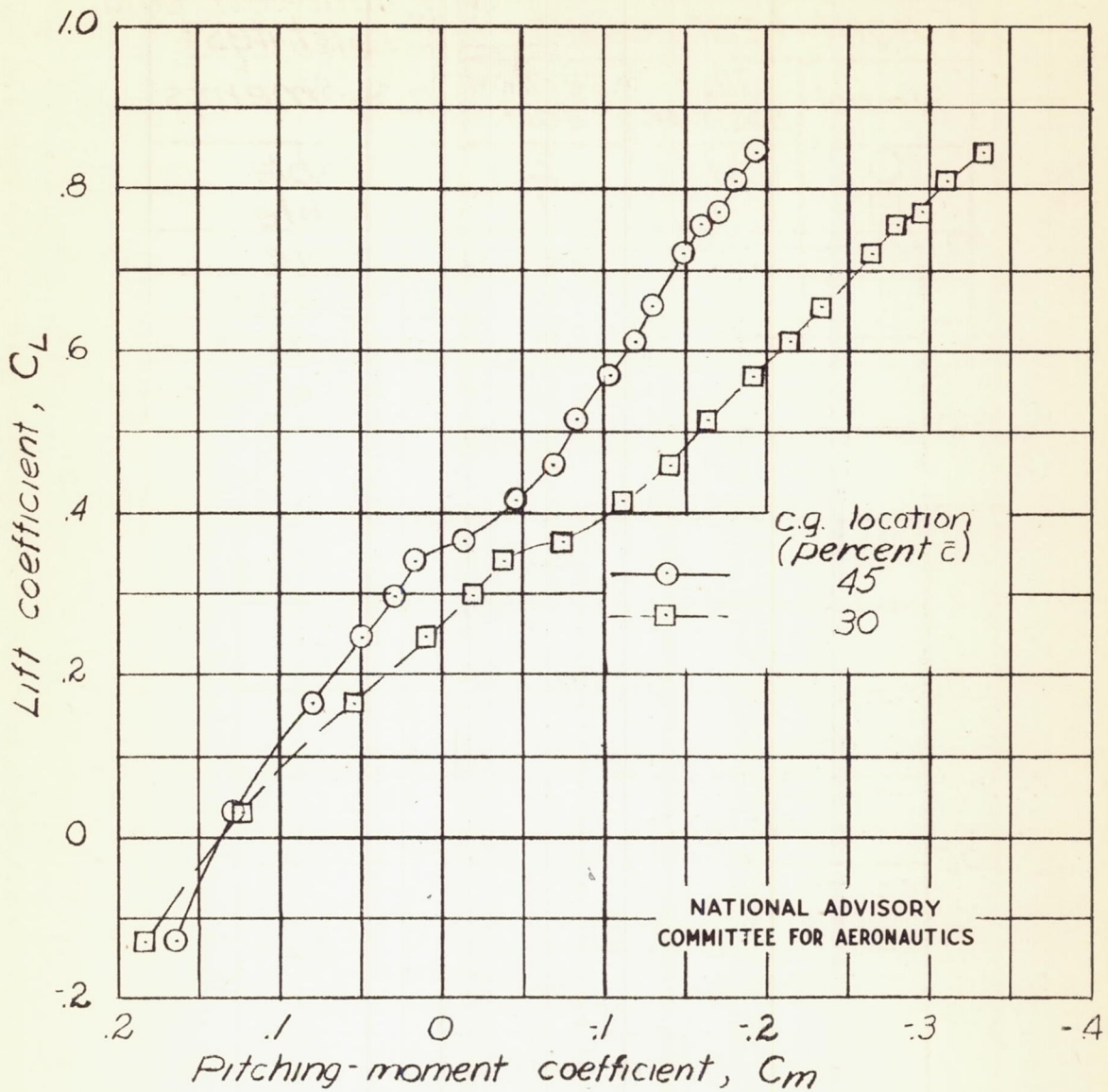
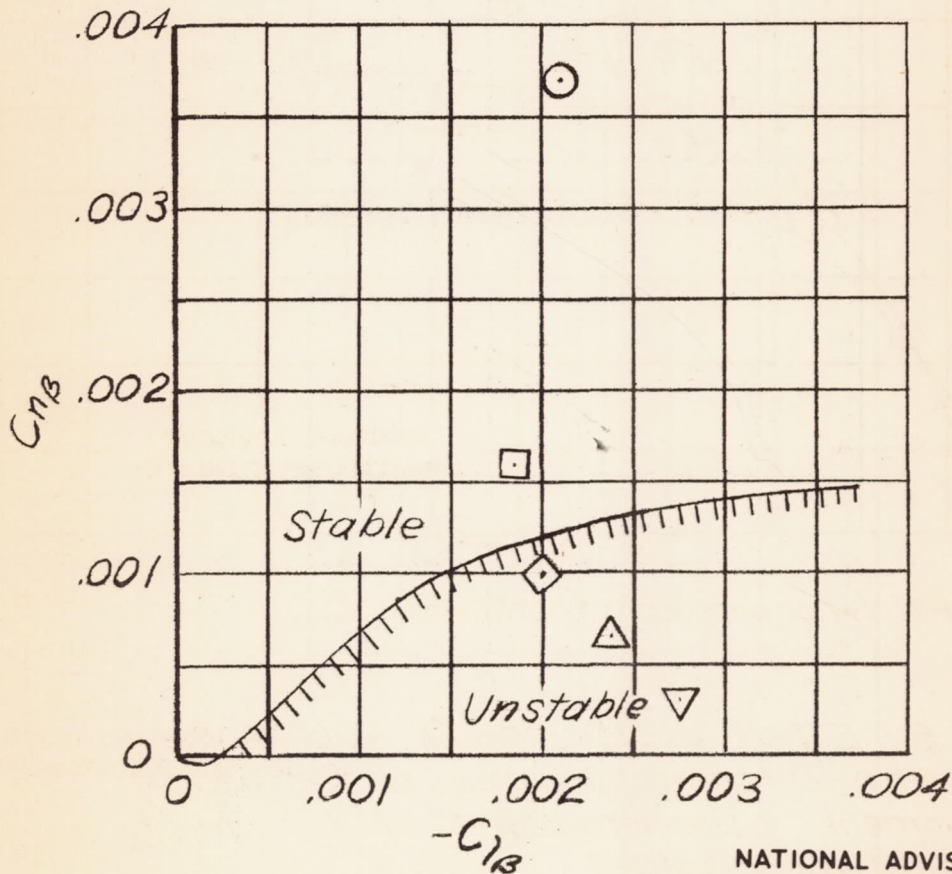


Figure 8.- Effect of 15-percent shift in the center-of-gravity location on the pitching-moment characteristics of a 62° swept-back-wing model.

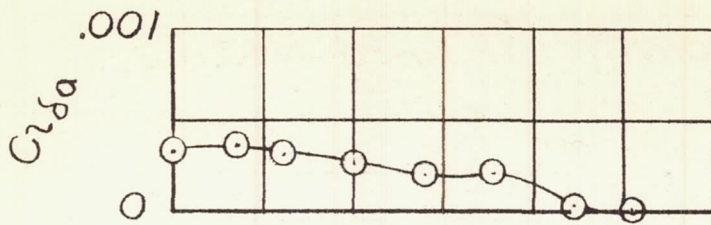
Flight-test points			Flight-test comments
Symbol	Test position	Vertical tail	
○	1	2	Stable
□	1	1	Stable
<sup>a</sup> ◇	2	1	Stable
△	3	1	Unflyable
▽	4	1	Unflyable

<sup>a</sup> $C_{n\beta}$  and  $Q_{\beta}$  interpolated from force-test data of figure 5.

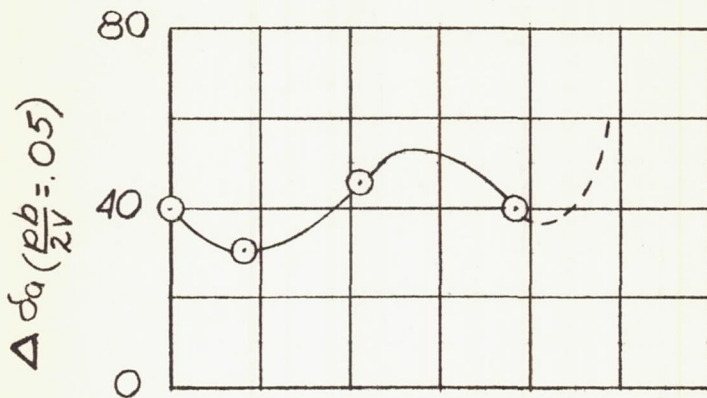


NATIONAL ADVISORY  
COMMITTEE FOR AERONAUTICS

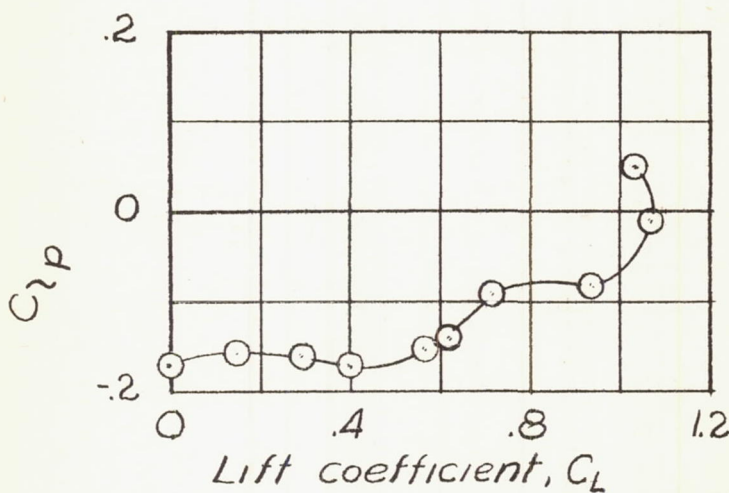
Figure 9.- Correlation of the calculated  $R=0$  boundary with flight-test results,  $C_L=0.6$ . (Product of inertia terms included in calculations.)



(a) Aileron effectiveness.



(b) Aileron rolling effectiveness.



(c) Damping in roll.

NATIONAL ADVISORY  
COMMITTEE FOR AERONAUTICS

Figure 10.- Variation of  $C_{lp}$ ,  $C_{l\delta a}$ , and  $\Delta\delta_a$  ( $\frac{pb}{2V} = .05$ ) with lift coefficient for the  $62^\circ$  swept-back wing. Data from reference 1.